

Combating multidrug-resistance in *S. pneumoniae*: a G-quadruplex binding inhibitor of efflux pump and its bio-orthogonal assembly

Ritapa Chaudhuri^{1,†}, Thumpati Prasanth^{1,†}, Debasmita Biswas¹, Subhranshu Mandal² and Jyotirmayee Dash^{1,*}

¹School of Chemical Sciences, Indian Association for the Cultivation of Science, Kolkata, West-Bengal 700032, India

²Laboratory Medicine, Chittaranjan National Cancer Institute, Kolkata, West Bengal 700156, India

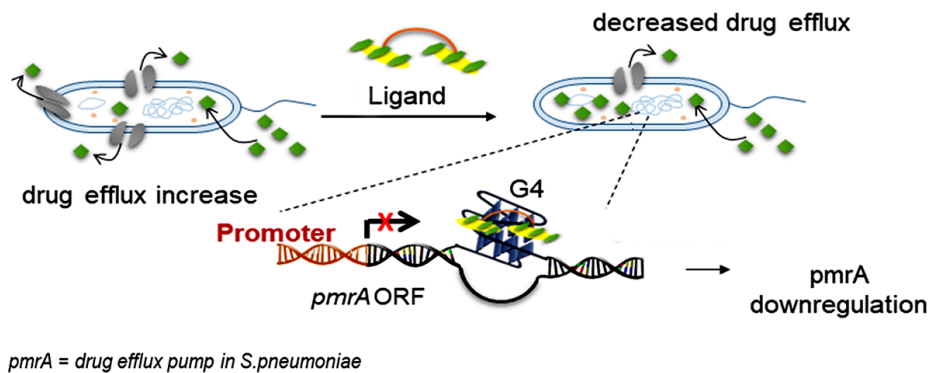
*To whom correspondence should be addressed. Tel: +91 33 2473 4971 (Ext. 1405); Email: ocjd@iacs.res.in

†The first two authors should be regarded as Joint First Authors.

Abstract

Antibiotic resistance poses a significant global health threat, necessitating innovative strategies to combat multidrug-resistant bacterial infections. *Streptococcus pneumoniae*, a pathogen responsible for various infections, harbors highly conserved DNA quadruplexes in genes linked to its pathogenesis. In this study, we introduce a novel approach to counter antibiotic resistance by stabilizing G-quadruplex structures within the open reading frames of key resistance-associated genes (*pmrA*, *recD* and *hsdS*). We synthesized **An4**, a bis-anthracene derivative, using Cu(I)-catalyzed azide-alkyne cycloaddition, which exhibited remarkable binding and stabilization of the G-quadruplex in the *pmrA* gene responsible for drug efflux. **An4** effectively permeated multidrug-resistant *S. pneumoniae* strains, leading to a substantial 12.5-fold reduction in ciprofloxacin resistance. Furthermore, **An4** downregulated *pmrA* gene expression, enhancing drug retention within bacterial cells. Remarkably, the *pmrA* G-quadruplex cloned into the pET28a(+) plasmid transformed into *Escherichia coli* BL21 cells can template Cu-free bio-orthogonal synthesis of **An4** from its corresponding alkyne and azide fragments. This study presents a pioneering strategy to combat antibiotic resistance by genetically reducing drug efflux pump expression through G-quadruplex stabilization, offering promising avenues for addressing antibiotic resistance.

Graphical abstract



Introduction

G-quadruplexes (G4s) are four-stranded DNA secondary structures that act as molecular switches in regulating key physiological processes (1–3). Their crucial role in telomere maintenance, oncogene expression, DNA replication etc., makes them important drug targets for anticancer therapeutics (4–7). Intriguingly, highly conserved G-quadruplex sequences have been identified throughout the genome of microbial organisms and are anticipated to play key roles in microbial propagation, gene regulation, recombination processes and pathogenesis (8–14). While many G4-binding small

molecules exhibit significant *in vitro* and *in vivo* anti-cancer activities (15,16), studies using small molecular probes to elucidate the functional role of G-quadruplexes in pathogens and their influence on pathogenicity are less studied to date (11,13,17–21). One of the earliest reports by Seifert and Cahoon showed that an intramolecular G-quadruplex formed near the *PilE* gene have a potential role in exhibiting antigenic variation in *Neisseria gonorrhoeae* (11). Nicolas *et al.* showed that bisquinolinium ligands Phen-DC 3 and Phen-DC 6 effectively binds G4s in *S. cerevisiae* triggering genetic instability (17). Cebrian *et al.* showed that

Received: December 18, 2023. Revised: March 26, 2024. Editorial Decision: April 2, 2024. Accepted: April 10, 2024

© The Author(s) 2024. Published by Oxford University Press on behalf of NAR Molecular Medicine.

This is an Open Access article distributed under the terms of the Creative Commons Attribution-NonCommercial License

(<https://creativecommons.org/licenses/by-nc/4.0/>), which permits non-commercial re-use, distribution, and reproduction in any medium, provided the original work is properly cited. For commercial re-use, please contact journals.permissions@oup.com

naphthalene diimide (NDI) ligands (known G4-binders) can modulate transcription in Gram-positive and Gram-negative bacteria through G-quadruplex stabilization (19). NDIs were also reported to influence gene expression in the parasite *T. brucei* through G-quadruplex stabilization (J. Med. Chem. 2018, 61, 1231–1240).

Streptococcus pneumoniae, primarily known for causing community acquired pneumonia (22), contains highly conserved G-quadruplex motifs in the open reading frames of three crucial genes, *pmrA*, *recD* and *hsdS*, involved in pathogenesis (23). The *pmrA* gene encodes for a trans-membrane protein, PmrA, one of the major facilitator superfamily of efflux pumps responsible for drug efflux in *S. pneumoniae* (24,25). Drug efflux, by which bacteria spontaneously throw out ingested anti-bacterial substances, is one of the major causes of antibiotic resistance. Fluoroquinolone resistance associated with PmrA has been well characterized in *S. pneumoniae* (24). Therefore, targeting the G-quadruplex in the *pmrA* gene will be an alternative strategy for combating drug resistance in *S. pneumoniae*. In addition to *pmrA*, highly conserved G4-forming motifs have been identified in *recD* and *hsdS* genes of *S. pneumoniae*, which are known to be involved in host-pathogen interactions (23). The *hsdS* gene has the putative G4 forming sequence in its coding region, vital in regulating the type 1 restriction-modification system. Depending on the host niche for facilitating infection, the *hsdS* gene is directly involved in controlling the interconversion of virulent to less-virulent phenotypes of *S. pneumoniae* (26). Conversely, the *recD* gene plays an essential role in the bacteria's DNA double-strand break repair mechanism (27). The formation of the G4 motif in the coding region of the *recD* gene hinders expression of the RecD protein leading to inhibition of the DNA recombination and repair mechanisms (23).

Given the increasing prevalence of resistance to traditional β -lactam antibiotics, there is an urgent need to develop novel therapeutic approaches to combat multidrug resistance (28–30). In this study, we have developed bis-anthracene derivatives designed to target G-quadruplexes (G4s) within three specific genes (*pmrA*, *recD* and *hsdS*) found in *Streptococcus pneumoniae*. We have evaluated the effect of these ligands on clinical isolates of multidrug-resistant (MDR) *S. pneumoniae*. Interestingly, the most potent ligand was synthesized through bioorthogonal cycloaddition within live bacterial cells that had been transformed with a plasmid containing the *pmrA*-G4 sequence.

Materials and methods

Identification of bacterial strains from clinical isolates

Bacteria from the patient's urine were cultured in a blood agar plate and incubated in 37°C incubator. Colonies (3–5 each) from the overnight culture plate were diluted in 0.45% NaCl buffer (pH ~ 4.5–7.2) to make a solution with 0.5 MCF turbidity. Bacterial solution (1 μ l) was then mixed with 1 μ l α -CHCA matrix. The sample mixture (2 μ l) was then dropped on MALDI 96 well plate dried and then placed into the ionization chamber of the mass spectrometer. Specific peaks corresponding to *m/z* values of different biomolecules were obtained. The software compares the obtained spectrum to the peak weights defined for each claimed species. A quantitative value, the confidence value, was calculated and expressed the

similarity between the unknown organism and every organism or organism group in the database. When no match was found, the organism was considered as non-identified. This method was employed to identify *Streptococcus pneumoniae*, *Klebsiella pneumoniae*, *Escherichia coli*, *Pseudomonas aeruginosa* and *Staphylococcus aureus*.

Antibiotic susceptibility analysis of the bacterial strains

The resistance of the clinically isolated bacterial strains towards different groups of antibiotics was evaluated using the clinical VITEK 2 drug-resistant diagnostic method (31). Bacterial strains were isolated from clinical samples (urine) and plated on blood agar plates according to the standard procedure. Colonies (3–5 each) from the overnight culture plates were diluted in 0.45% NaCl buffer (pH ~ 4.5–7.2) to make a solution of 0.5 MCF turbidity. Then, a 20-fold dilution was made and dispensed into the reagent card (for e.g. AST ST03 for *S. pneumoniae* drug-resistant testing card) for automatic reading by the VITEK 2 Compact system to obtain drug resistant information.

Minimal inhibitory concentrations (MIC)

The antibacterial property of the ligands was evaluated by determining the minimum inhibitory concentration or MIC using broth microdilution assay. Antibacterial properties of the bis-anthracene ligands were determined against Gram-positive (*S. aureus*, *S. pneumoniae*) and Gram-negative (*E. coli*, *P. aeruginosa* and *K. pneumoniae*) bacteria. Different bacterial strains were cultured overnight in suitable media containing $\sim 10^9$ CFU ml⁻¹ (determined by spread plating method). 1.5% of the overnight grown primary culture was inoculated in fresh appropriate media at 180 rpm, 37°C and allowed to grow to 0.5 MCF turbidity (log phase). 5 μ l of the log phase cells was mixed in 5 ml fresh media and 200 μ l of the suspension from the mixture was transferred to each well of the 96-well plate. The bacterial suspensions were then inoculated with increasing concentrations of the ligands up to 800 μ M. The same was also done in combination with standardized amount of ciprofloxacin. Negative control containing 200 μ l of only fresh media and positive control containing bacterial suspension and ampicillin were also kept. The suspensions were then incubated at 37°C for a period of 12–16 h and the O.D. values, measured at 600 nm using a multiscan FC ELISA reader (Thermo Scientific). The experiment was performed in triplicates and MIC values reported are an average of the data obtained.

Fractional inhibitory concentration (FIC): For two antimicrobial agents, P and Q, here P refers to ciprofloxacin and Q refers to An4, the FICI index is calculated by adding FIC_P with FIC_Q, as follows:

$$FICI = FIC_P + FIC_Q$$

Here,

$$FIC_P = \frac{\text{MIC of P in presence of Q}}{\text{MIC of P alone}} = \frac{14}{80} = 0.17$$

$$FIC_Q = \frac{\text{MIC of Q in presence of P}}{\text{MIC of Q alone}} = \frac{4}{50} = 0.08$$

Therefore, the FICI is 0.25 indicating synergistic activity of ciprofloxacin and An4.

FRET melting studies

Dual labeled DNA sequences (see S.I. for details) with a donor 5'-FAM (fluorophore 6-carboxyfluorescein; $\lambda_{\text{ex}} \sim 490$ nm/ $\lambda_{\text{em}} \sim 520$ nm) and an acceptor fluorophore 3'-TAMRA (6-carboxytetramethylrhodamine; $\lambda_{\text{ex}} \sim 555$ nm/ $\lambda_{\text{em}} \sim 580$ nm) were first diluted to 400 nM using a 60 mM potassium cacodylate (K-Caco, pH 7.4) buffer and annealed by heating to 95°C for 5 min followed by slow cooling to room temperature and then incubated overnight at 4°C. Subsequently, sample solutions were prepared in Roche 96-well plate (with a total volume of 100 μ l) by mixing the pre-annealed DNA (at 200 nM final concentration) with ligands **An1**, **An2**, **An3**, **An4** (0–10 equivalent) in 60 mM potassium cacodylate, pH \sim 7.4 and incubated in dark for 1 h. Measurements were made in triplicate with excitation at 483 nm and detection at 533 nm. Melting curves for the determination of melting temperature (T_m) were then obtained by recording FAM fluorescence with increasing temperatures from 37 to 95°C at the rate of 0.9°C/min using Roche Light Cycler II. The analysis of T_m values was accomplished using OriginPro 2018 software.

Fluorimetric titrations

Fluorescence spectroscopic titrations were recorded in Horiba Jobin Yvon Fluoromax 3 instrument at 25°C using a 1 mm quartz cuvette. Fluorimetric titrations were performed with successive addition of the pre-annealed DNA (See S.I. for details) solution into the 1 μ M ligand solution in 100 mM Tris-KCl buffer, pH \sim 7.4. The emission of **An1–An4** was measured from the wavelength range of 350–500 nm.

The following Hill equation was used to calculate the dissociation constants.

$$F = F_0 + \frac{(F_{\text{max}} - F_0)[\text{DNA}]}{K_D + [\text{DNA}]}$$

where F denotes fluorescence intensity, F_{max} for maximum fluorescence, F_0 for fluorescence in the absence of DNA and K_D indicates dissociation constant.

Isothermal titration calorimetry (ITC)

ITC experiments were conducted in MicroCal PEAQ-ITC (Malvern, USA) microcalorimeter. DNA sequences were pre-annealed in 100 mM potassium chloride buffer (pH \sim 7.4) by heating in a dry bath to 95°C for 5 min followed by slow cooling at 25°C and incubated overnight at 4°C. The reference cell was filled with 100 mM KCl buffer (pH \sim 7.4). The pre-annealed DNA G-quadruplex (2.5 μ M) in buffer was kept in the sample cell and the ligands (25 μ M) were filled in the syringe of volume 40 μ l in the same buffer. Ligand solution was added sequentially, mixing was carried out by stirring the syringe at a speed of 750 rpm at 298 K. 30 injections with duration of 2.6 and 100 s of spacing between two injections were set up. Blank titrations were conducted by injecting the ligand into the cell containing only buffer under the same conditions. The heat generated due to interaction was determined by subtracting the blank heat from that for the ligand–DNA titration. The raw data were analyzed using the Malvern ITC Analysis software provided with the instrument. The data fitting was done using an appropriate binding model.

Cell viability analysis using XTT assay

Adult human normal kidney epithelial (NKE) cells were cultured using RPMI 1640 containing 10% FBS, 1% penicillin–

streptomycin. The NKE cells were cultured at 37°C in a 5% carbon dioxide (CO₂)/95% air atmosphere. Cytotoxicity of different ligands in human normal kidney epithelial cells was evaluated using XTT assay. XTT (Invitrogen) is a colorless or slightly yellow compound which is metabolically reduced to give bright orange colour in live cells. The NKE cells were then treated with increasing concentrations (up to 100 μ M) of bis-anthracene ligands and incubated for 24 h. 25 μ l Solution containing 1mg/ml of XTT and 3 mg/ml of PMS were added to 100 μ l of cell culture medium into each well of 96-well plate. PMS enhances the reduction reaction for better detection. Absorbance (A) of formazan dye was recorded at 450 nm using a micro plate reader. The percentage of viable cells was determined by the following equation. The final IC₅₀ values of each ligand were calculated by using the OriginPro 2018.

$$\text{Viable cells (\%)} = \frac{\text{Absorbance of treated cells}}{\text{Absorbance of untreated cells}} \times 100$$

Confocal imaging

A single colony of the MDR *S. pneumoniae* was inoculated into fresh TSB and allowed to grow overnight at 37°C and 180 rpm. 1.5% of the primary culture was inoculated in fresh appropriate media at 180 rpm, 37°C and allowed to grow to 0.5 MCF turbidity (log phase). Log phase cells were then treated with 20 μ M ligand **An4** (less than MIC concentration) and kept overnight at 37°C. The cells were centrifuged at 4000g for 5 min and washed with 1 \times PBS twice. 4% Paraformaldehyde was used for fixing the cells and they were washed again twice with 1 \times PBS. Finally, the bacterial cell pellet was dissolved in 200 μ l 1 \times PBS and mounted on glass slide with antifade solution (ProLong Gold Antifade Mountant). The sample was visualized using Leica DMI8 Stellaris 5 microscope.

RNA extraction and qRT-PCR

A single colony of the clinical isolate of *S. pneumoniae* was inoculated into fresh TSB (Tryptone Soya Broth; Himedia M011) and allowed to grow overnight at 37°C and 180 rpm. 1.5% of the primary culture was inoculated in fresh appropriate media at 180 rpm, 37°C and allowed to grow to 0.5 MCF turbidity (log phase). The log phase cells were divided into 4 tubes, and then one was treated with ligand **An4** only, another with ciprofloxacin only, the third one with both **An4** and ciprofloxacin, and the last one was kept untreated. After overnight incubation, total RNA was isolated using HiPurA Bacterial RNA Purification Kit (Himedia) according to the manufacturer's instructions. RNA quantification was carried out by a Cary Win 300 UV-Vis spectrophotometer. The total 500 ng of RNA was employed as a template for cDNA synthesis using a Verso kit (Thermo Fisher Scientific) as per the supplied protocol. Real-time PCR was carried out on Roche LightCycler 480 by the use of SYBR Premix (Roche), according to the manufacturer's instructions. The C_t method (comparative cycle threshold method) was used to calculate relative mRNA expression. The C_t values were normalized to 16s rRNA and compared to the untreated cells. The quantification was performed in triplicates. The significance level was statistically analyzed by employing a Student's t test, and the results were statistically significant when $*P < 0.05$.

eGFP reporter assay

The overnight-grown primary culture (1.5%) of *pmrA*-eGFP_pET28a (+) transformed *E. coli* BL21 cells was seeded in fresh Luria Bertini Broth and allowed to grow to 0.5 MCF turbidity (log phase) at 180 rpm, 37°C. Cells were then treated with 5 µg/ml and 10 µg/ml ligand **An4** (less than MIC concentration) and incubated for 6 h at 30–37°C. After incubation, the cells were induced with 0.5 mM IPTG (isopropyl β-D-1-thiogalactopyranoside) for 3–4 h. The induced cells were used for total RNA extraction. RNA isolation was performed using HiPurA Bacterial RNA Purification Kit (Himedia) according to the manufacturer's instructions. RNA quantification was carried out by a Cary Win 300 UV-Vis spectrophotometer and the total 500 ng of RNA was employed as a template for cDNA synthesis using a Verso kit (Thermo Fisher Scientific) as per the supplied protocol. Real-time PCR was carried out on Roche LightCycler 480 by the use of SYBR Premix (Roche), according to the manufacturer's instructions. The C_t method (comparative cycle threshold method) was used to calculate relative mRNA expression. The C_t values were normalized to 16 s rRNA and compared to the untreated cells. The quantification was performed in triplicates. The significance level was statistically analyzed by employing a Student's *t* test, and results were statistically significant when $*P < 0.05$.

SIMS analysis

ToF-SIMS experiments were carried out in a Ion-TOF TOF-SIMS 5–100 manufactured by Münster, Germany, equipped with a Bi LMIG and GCIB Ar electron impact source. Bacterial cells (2 ml) grown till 0.5 MCF were treated with ligand **An4** (5 and 10 µg/ml) for 16 h. The cells were then washed with PBS and again treated with EtBr (0.5 µg/ml) for 2 h at 0.5 MCF turbidity to ensure equal distribution of bacteria. Excess EtBr was removed by successive washing steps using $1 \times$ PBS. The cells were resuspended in 200 µl PBS and mounted on clean glass slides. The sample was air dried and kept in the desiccator for 24 h prior to ToF-SIMS analysis (see S.I. for details).

Results and discussions

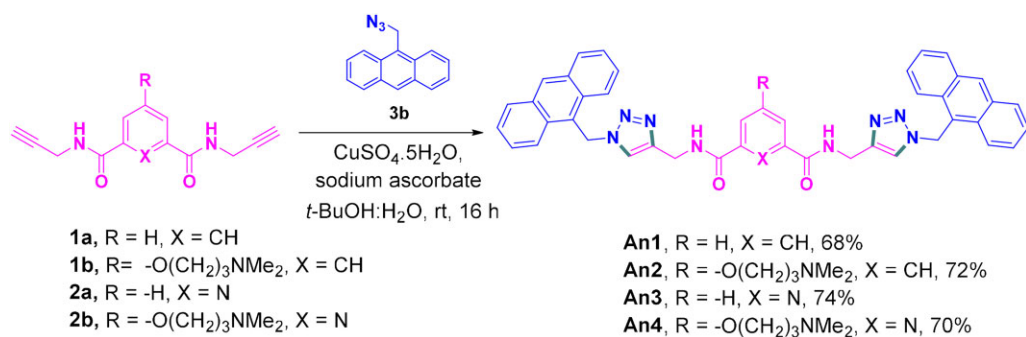
We employed a Cu(I)-catalyzed azide-alkyne cycloaddition reaction between an anthracene-based azide compound and bis-alkynes derived from pyridine and benzene dicarboxamides to synthesize bis-anthracene ligands (as shown in Scheme 1). These ligands feature extended aromatic anthracene motifs that are anticipated to engage in π -stacking interactions with the G-quartet structure of G4 DNA. Additionally, the triazole heterocycles offer a wide range of pharmacological properties, including antimicrobial effects. (32) Moreover, the peptidomimetic backbone of these ligands, along with their alkyl amine side chains, may facilitate their permeability through the bacterial cell wall.

First, we evaluated the ability of these ligands to stabilize G-quadruplex structures (G4s) located within the open reading frames (ORF) of the *pmrA*, *recD* and *hsdS* genes in *S. pneumoniae* using the FRET-based melting assay (34). The stabilization potential of bis-anthracene ligands **An1–An4** was determined by measuring the emission of the donor (FAM) in 5 FAM and 3 TAMRA labeled G4 sequences (*pmrA*, *recD*, *hsdS*) and *dsDNA* with increasing temperature. It was observed that **An4** effectively stabilized the *pmrA* G4 struc-

ture compared to other G4s and *dsDNA* (Figure 1A and B, Supplementary Figure S1–S5), with a ΔT_m value of 7°C at a 5 µM concentration. In contrast, **An2** raised the melting temperature of the *hsdS* G4 by 10°C at the same concentration. Thus, water soluble methyl-amine side-chains present in **An2** and **An4** contributes to the thermal stabilization of the *pmrA* and *hsdS* G-quadruplexes. However, ligands **An1** and **An3** lacking the side-chain did not significantly stabilize the G4s or duplex DNA.

Subsequent fluorimetric titrations of the ligands with G4 DNAs validate the observations from FRET melting assay. (Figure 1C–D, Supplementary Figure S6–S10). Ligands **An1–An4**, owing to the presence of the UV-active anthracene moiety, displayed distinct emission bands at 396, 418 and 441 nm when excited at 320 nm. Among them, **An4** exhibited remarkable fluorescence enhancements and displayed the highest binding affinity towards the *pmrA* G4, with a K_d value of 0.6 µM, accompanied by a 10 nm red-shift. **An2** exhibited higher affinity for the *hsdS* G4 compared to *pmrA* and *recD* G4s. However, none of the ligands exhibited binding to *dsDNA* or human telomeric G-quadruplex DNA, indicating a lower chance of cross-reactivity with human G4 DNAs. Ligands **An1** and **An3** did not exhibit significant binding to any of the DNAs considered in this study. As **An2** showed insignificant anti-bacterial activity even in the presence of ciprofloxacin, it was excluded from further studies. **An4**, which showed selectivity towards the *pmrA* G-quadruplex, was subjected to detailed analysis of molecular interactions using isothermal calorimetry. The thermograms obtained upon titration of the three G-quadruplexes with **An4** displayed exothermic peaks, suggesting intercalation of the bis-anthracene ligands into the G4 DNAs, due to π - π stacking interactions with the DNA bases. **An4** exhibited the highest binding affinity for *pmrA* ($K_d = 1.9$ µM, $\Delta H = -80$ kcal/mol) with a 1:1 stoichiometry (Figure 1E). It displayed lower binding affinity towards *recD* ($K_d \sim 6$ µM) and *hsdS* ($K_d \sim 5$ µM) G4 DNAs (Supplementary Figure S11). The thermodynamic findings helped us gain insights of the binding ability of the ligand **An4** to the three G4s. Comparing the K_d and enthalpy (ΔH) values from the ITC thermogram data of *recD* and *hsdS* to those of *pmrA* indicated that **An4** exhibits stronger binding to the *pmrA* G4. Thus, *recD* and *hsdS* were excluded from further experiments. Nevertheless, these G4s have much biological importance and could emerge as potential targets for drug development in the future. However, no binding data of **An4** could be extracted from the scattered plot obtained with *dsDNA*, suggesting no significant interaction between them.

The antibacterial efficacy of the bis-anthracene ligands was simultaneously assessed using a minimum inhibitory concentration (MIC) assay against clinical isolates of *S. pneumoniae* strains, and the results are summarized in Table 1. Additionally, these compounds were also tested against other pathogenic strains, including *K. pneumoniae*, *E. coli*, *P. aeruginosa* and *S. aureus* (Table 1). The clinical bacterial strains were identified using the automated VITEK MALDI-TOF MS system (manufactured by Biomerieux.). The antibiotic susceptibility profiles for each strain were determined using the automated Vitek 2 Compact system, which reveals that these bacterial strains exhibit resistance to a variety of antibiotics (see Supporting Information, Supplementary Table S1). The MIC values of bis-anthracene ligands against *S. pneumoniae*, showed moderate antibacterial activity with ligand **An4** exhibiting a comparatively lower MIC of 80 µg/ml. However,



Scheme 1. Chemical synthesis of bis-anthracene derivatives (An1–An4) by Cu(I)-catalyzed azide–alkyne cycloaddition.

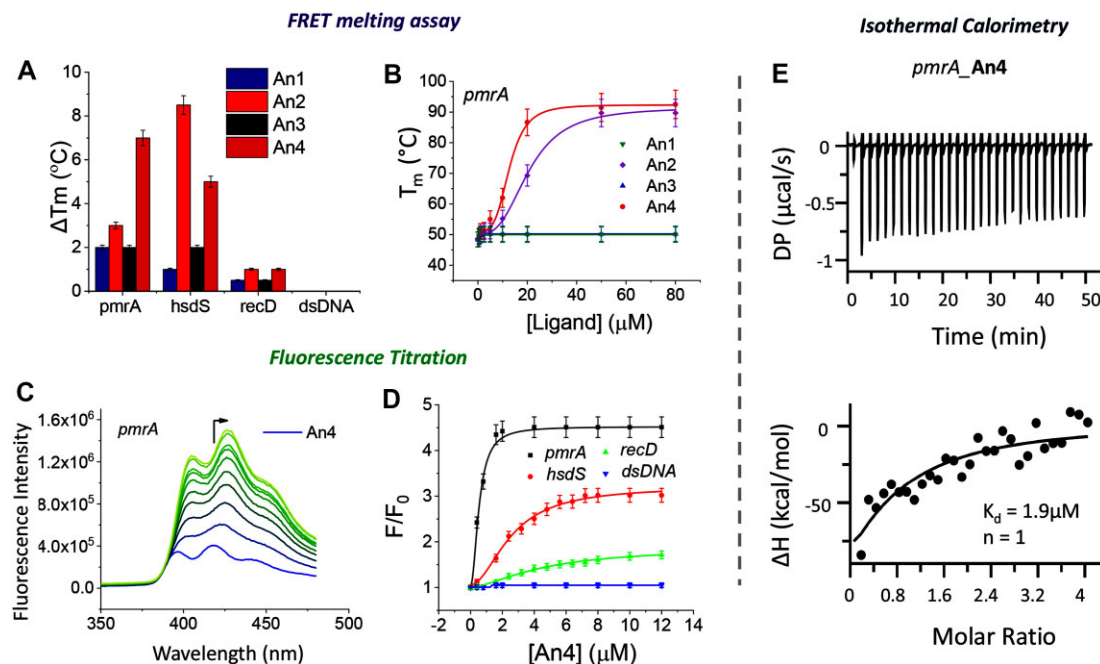


Figure 1. (A) Stabilization potential (ΔT_m) of bis-anthracene derivatives (**An1–An4**) at 5 μM concentration for *pmrA*, *recD*, *hsdS* G4 and dsDNA analyzed by FRET melting assay. (B) Melting curve of *pmrA* G4 DNA in the presence of **An1–An4**. (C) Fluorescence spectroscopic titrations of ligand **An4** (1 μM) with *pmrA* G4 DNA. (D) Fluorescence response curves of An4 upon titration with *pmrA*, *recD*, *hsdS* G4 and duplex DNA. (E) Isothermal calorimetric titration of *pmrA* G-quadruplex with **An4**; heat-burst curve (upper panel) and binding isotherm profile (lower panel).

these ligands exhibited notably reduced antibacterial activity against multidrug-resistant *S. pneumoniae* strains (Table 1).

To evaluate their combined impact, we co-administered ciprofloxacin with the newly synthesized anthracene ligands (**An1–An4**) in *S. pneumoniae* cultures with a turbidity of 0.5 MCF. Ligand **An4** enhanced the antibiotic activity of ciprofloxacin, reducing its MIC value to 4 $\mu\text{g}/\text{ml}$, a substantial 12.5-fold improvement. However, **An1**, **An2** and **An3** did not exhibit a similar reduction in ciprofloxacin resistance in *S. pneumoniae* (Figure 2A).

Next, we determined the fractional inhibitory concentration indices (FICI) (33) to assess the synergistic effect of ligand **An4** when combined with ciprofloxacin against the multidrug-resistant (MDR) strain of *S. pneumoniae*. The resulting FICI value of 0.25 indicated a synergistic interaction between **An4** and ciprofloxacin. ($\text{FIC} \leq 0.25$ denotes synergism, while $0.25 < \text{FICI} < 2$ suggests indifference, and $\text{FIC} \geq 2$ implies antagonism).

To assess the cellular toxicity of the ligands for potential use as antibacterial agents, an XTT assay was conducted us-

ing **An1–An4** on normal human kidney epithelial (NKE) cells. Results indicated that all ligands were non-toxic, and IC_{50} values could not be determined even at a concentration of 80 $\mu\text{g}/\text{ml}$ in human NKE cells (Supplementary Figure S12). Furthermore, confocal microscopy was employed to visualize the localization of **An4** in *S. pneumoniae*. Bacterial cells in the logarithmic growth phase (O.D. ~ 0.4 – 0.6) were treated with 5 $\mu\text{g}/\text{ml}$ of **An4**, a concentration below its MIC_{50} value, for 3 h at 37°C. After washing with PBS, the cells were resuspended in an anti-fade solution and mounted on glass slides with coverslips before confocal imaging. The intense fluorescent blue color observed in *S. pneumoniae* confirmed the permeability of **An4** through the cell wall of the Gram-positive bacteria (Figure 2B). To gain insights into **An4**'s antibacterial mechanism, we first evaluated whether the clinically isolated strain of *S. pneumoniae* could indeed express the *pmrA* gene by qRT-PCR assay. We observed that the *S. pneumoniae* strain could significantly express the *pmrA* gene ($C_t \sim 20$), calculated after normalization to 16s rRNA. Subsequently, we investigated the effect of ciprofloxacin and **An4** in reducing the expression

Table 1. The MIC values of **An1–An4** against a range of pathogenic clinical isolates of *E. coli*, *K. pneumoniae*, *P. aeruginosa*, *B. cereus* and *S. pneumoniae*

	<i>E. coli</i> ($\mu\text{g/ml}$)	<i>K. pneumoniae</i> ($\mu\text{g/ml}$)	<i>P. aeruginosa</i> ($\mu\text{g/ml}$)	<i>S. aureus</i> ($\mu\text{g/ml}$)	<i>S. pneumoniae</i> ($\mu\text{g/ml}$)
An1	350	350	>700	350	350
An2	>800	>800	>800	640	160
An3	>560	>700	>700	560	140
An4	640	>800	400	640	80

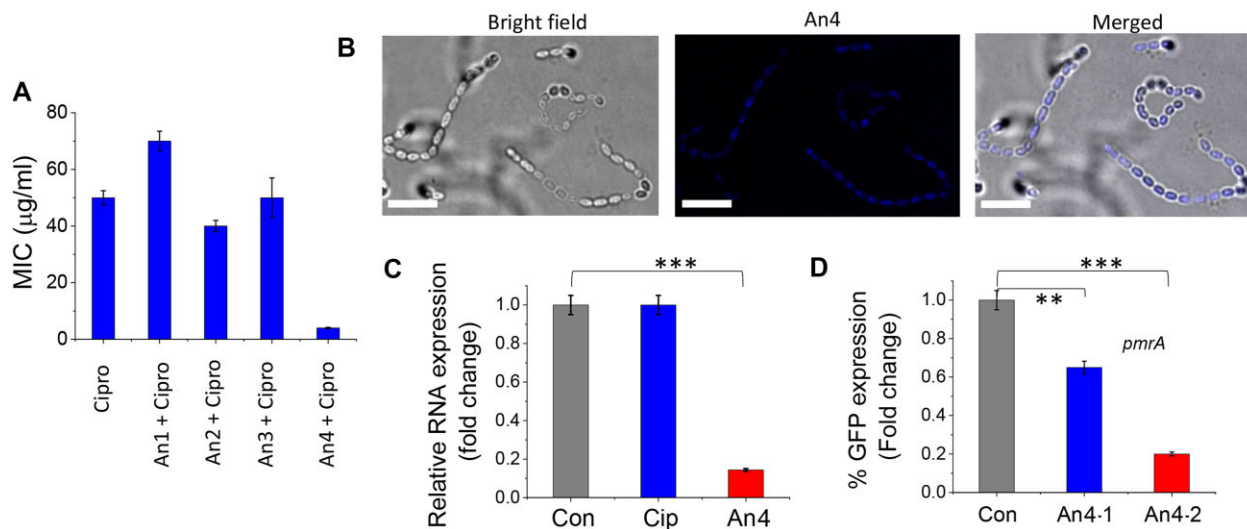


Figure 2. (A) Determination of MIC of ciprofloxacin, **An4**, and ciprofloxacin combined with 10 $\mu\text{g/ml}$ **An4** against MDR strain of *S. pneumoniae*. (B) Confocal images of *S. pneumoniae* showing cellular localization of **An4**, panel (i) bright field image of *S. pneumoniae*, panel (ii) image of *S. pneumoniae* in blue filter and panel (iii) merged image of panels i and ii; scale bar $\sim 10 \mu\text{m}$; DMI8 Stellaris 5 microscope. (C) Normalized fold change in expression of *pmrA* gene upon treatment with **An4** (10 μM) and ciprofloxacin in MDR *S. pneumoniae*. (D) Relative GFP expression upon binding of **An4** to *pmrA* G-quadruplex formed in the *pmrA* gene cloned upstream of the eGFP gene in *pmrA*-eGFP_pET28a(+) vector. Data are shown as mean values \pm SD of three independent samples. The asterisks denote statistically significant differences from control ** $P < 0.001$, *** $P < 0.0001$ (Student's *t* test).

of the *pmrA* gene using qRT-PCR. *S. pneumoniae* cells were treated with ciprofloxacin and **An4** for 16 h, and the total RNA was isolated, reverse transcribed to cDNA and quantified by real-time SYBR Green PCR assay. The results indicated that cells treated with ciprofloxacin exhibited no substantial impact on *pmrA* mRNA expression, whereas cells treated with **An4** demonstrated a remarkable 86% reduction in expression (as shown in Figure 2C and Supplementary Figure S13). This data explains the rationale behind the higher MIC of **An4** when administered alone compared to when used in combination with ciprofloxacin. **An4** exerts its antibacterial effects by inhibiting the expression of the drug efflux pump in drug-resistant *S. pneumoniae*. Consequently, this leads to increased intracellular retention of ciprofloxacin within *S. pneumoniae*, enhancing its antibiotic efficacy.

Subsequently, a GFP-based reporter assay confirming that the observed inhibition of *pmrA* expression results from **An4**'s G-quadruplex stabilization was performed. (35) There are instances of hindrance in the movement of transcriptional or translational machinery due to the formation and stabilization of a G-quadruplex structure in the promoter/ORF/UTR of a gene (36). We, then designed a reporter vector by incorporating the *pmrA* G-quadruplex-forming sequence immediately upstream of an eGFP gene within the pET28a(+) plasmid. The *pmrA*-eGFP_pET28a(+) vector was introduced into *E. coli* BL21 cells to facilitate GFP expression (Supplementary Figure S14A). The changes in GFP expression due to binding of **An4** to the *pmrA* G-quadruplex was mon-

itored by qRT-PCR analysis. Notably, it was observed that **An4** reduced a dose-dependent reduction in GFP RNA expression (normalized using 16s rRNA as a house-keeping gene), reducing it by 36% and by 80% at 5 and 10 $\mu\text{g/ml}$, respectively (Figure 2D and Supplementary Figure S14B). However, it's worth mentioning that ligand **An4** did not influence GFP expression in *E. coli* transformed with a control GFP vector that lacked the *pmrA* G4 element (Supplementary Figure S15). Therefore, these changes in GFP reporter expression in the presence of **An4** was also cross validated using fluorescence imaging (Supplementary Figure S16). Therefore, based on these findings, it can be deduced that the reduction in GFP expression is a consequence of transcriptional hindrance resulting from the **An4**-mediated stabilization of the *pmrA* G-quadruplex located immediately upstream of the GFP reporter gene. The images demonstrated a dose-dependent reduction in GFP expression in *pmrA*-eGFP_pET28a(+) transformed *E. coli* cells compared to control cells transformed with eGFP_pET28a(+) lacking the *pmrA* construct. These observations suggest that the decrease in GFP expression is attributed to transcriptional hindrance, caused by the **An4**-mediated stabilization of the *pmrA* G-quadruplex located immediately upstream of the GFP reporter gene.

To assess drug retention in multidrug-resistant (MDR) *S. pneumoniae* following *pmrA* inhibition, we employed spectral scanning and 2D time-of-flight secondary ion mass spectrometry (ToF-SIMS). (37) Bacterial cells were cultured to a turbidity of 0.5 MCF and treated with 5 $\mu\text{g/ml}$ of **An4**.

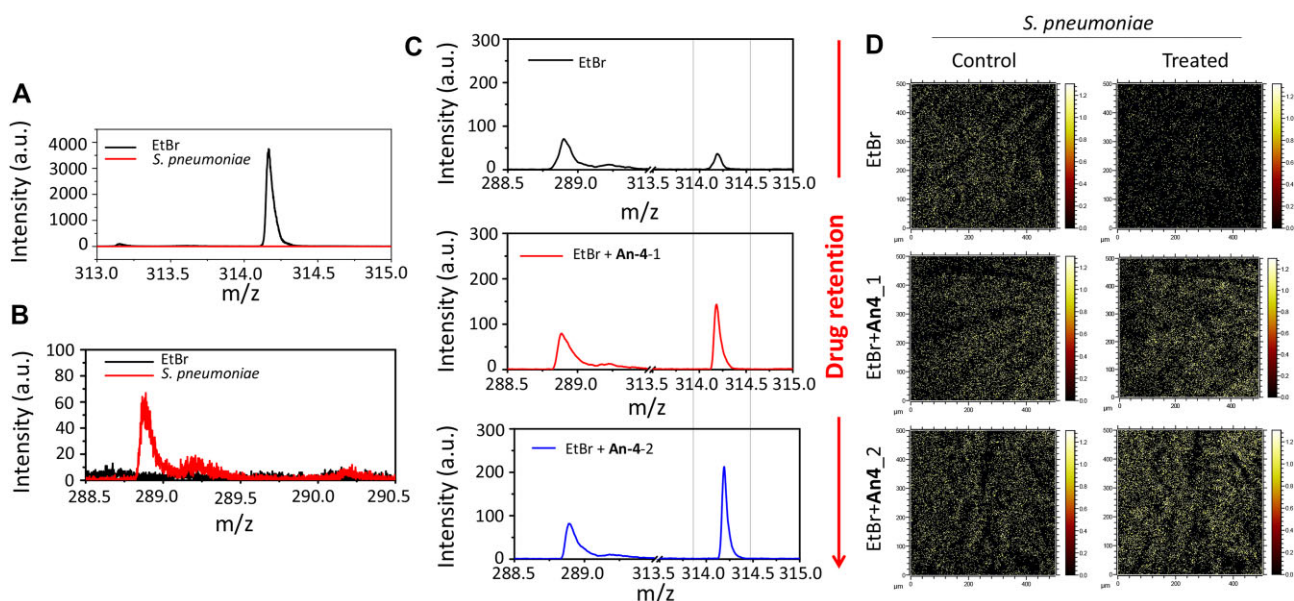
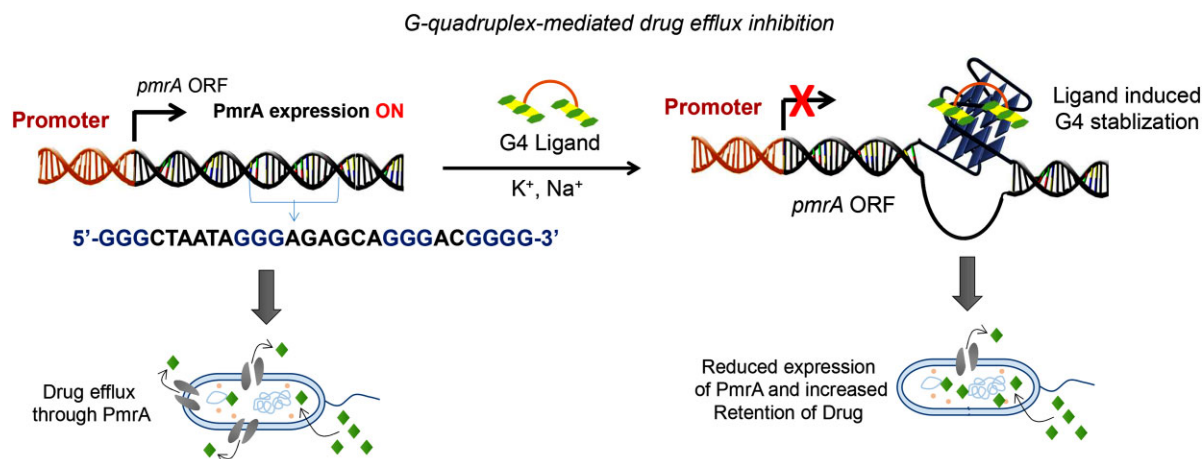


Figure 3. ToF-SIMS analysis, positive ion spectra corresponding to specific fragment of (A) EtBr drug (m/z value ~ 314.2) and (B) *S. pneumoniae* bacterial film ($m/z \sim 288.9$). (C) Positive ion spectra showing the increase in intensity of m/z peak at 314.3 with increasing the concentration of **An4** (0, 5 and 10 $\mu\text{g/ml}$, respectively) in bacterial treatment, and (D) ToF-SIMS images of EtBr ions ($m/z \sim 314.2$) in **An4** (5 and 10 $\mu\text{g/ml}$) treated *S. pneumoniae* bacterial films suggesting the retention of EtBr in *S. pneumoniae*.



Scheme 2. Proposed mechanism of G-quadruplex-mediated drug-efflux inhibition. The drug efflux pump gene *pmrA* is normally overexpressed in MDR *S. pneumoniae*. However the G-quadruplex present in the open-reading frame of *pmrA* presents a hindrance to the transcriptional machinery. Bis-anthracene ligands reduces *pmrA* gene expression by stabilizing the *pmrA*-G4s; thereby increases drug retention in the bacteria.

After 24 h, cells were exposed to ethidium bromide (EtBr) for 2 h, followed by thorough washing before sample preparation. We evaluated EtBr retention in the MDR bacteria by measuring the intensity of EtBr fragment ion peaks in SIMS-based spectra. EtBr, with a prominent mass (m/z) intensity peak at 314.18, distinct from *S. pneumoniae* characteristic peaks, enabled clear mapping of its distribution across the bacteria (Figure 3A). A mass peak at 288.89 was observed as one of the major peaks of *S. pneumoniae*, and its intensity was kept constant throughout the experiment for accurate EtBr detection in a fixed population of bacteria (Figure 3B). The surface ion densities increased approximately fourfold and six fold with increasing **An4** concentration of 5 $\mu\text{g/ml}$ and 10 $\mu\text{g/ml}$, respectively, compared to the untreated control (Figure 3C). Furthermore, the distribution of the product ions was investigated by MS/MS ion images. The surface ion density and 3D images for mass peak 314.18

demonstrated a dose-dependent increase in EtBr concentration within *S. pneumoniae* as the **An4** concentration increased (Figure 3D and Supplementary Figure S17). This observation aligns with the proposed mechanism for overcoming antibiotic resistance, wherein **An4**-mediated *pmrA* G-quadruplex stabilization leads to the inhibition of drug efflux. Consequently, this inhibition results in higher retention of the antibiotic ciprofloxacin in *S. pneumoniae* (Scheme 2).

Bio-orthogonal reactions were first carried out in bacteria by Bertozzi *et al.* to understand the peptidoglycan dynamics by metabolically inserting synthetic azidosugar (one of its components) followed by visualization using covalent reactions with click chemistry (38,39). Following this discovery, click chemistry has been extensively applied to bacteria to label carbohydrates (38,40–42), lipid (43,44), DNA (45) and proteins (46,47). Recently we have shown Cu-free macrocyclization of bisazide and bisalkyne fragments in live HeLa cells

using endogenous G-quadruplexes as target templates. (48) Since **An4** was identified as an excellent G-quadruplex binder, we thought of executing bio-orthogonal synthesis of **An4** using *pmrA* G-quadruplex as the template. First, we tried to synthesize **An4** by incubating *S. pneumoniae* with the corresponding alkyne **2b** and azide **3b** building fragments of **An4**. However, ESI-MS analysis of azide-alkyne-treated *S. pneumoniae* cell lysate produced no detectable peaks corresponding to **An4**. Next, the pET28a (+) plasmid containing the *pmrA* G-quadruplex forming sequence was transformed into *E. coli* BL21 cells. The cells were grown till 0.5 MCF turbidity and were treated with **2b** and **3b** in 1:5 ratio for 24 h. Cells were lysed with lysozyme, and the lysate was centrifuged at 6000 rpm. ESI-MS analysis of the supernatant revealed the presence of **An4**, indicating its bioorthogonal synthesis in living bacterial cells (Supplementary Figure S18). No *m/z* corresponding to **An4** was observed for untreated control.

In summary, we have introduced a novel strategy to combat antibiotic resistance by modulating the expression of a drug efflux pump (PmrA) in multidrug-resistant (MDR) *S. pneumoniae*. This was achieved through the stabilization of G-quadruplex DNA present within the ORF of *pmrA* gene. We synthesized a series of bis-anthracene derivatives (**An1–An4**), with **An4** displaying significant binding affinity for the *pmrA* G-quadruplex DNA, over other G-quadruplexes, human telomeric G4-DNA, and dsDNA. **An4** exhibited a moderate MIC against MDR *S. pneumoniae*; however, when combined with ciprofloxacin, it remarkably reduced the MIC of ciprofloxacin by 12.5-fold. Although these molecules did not show any impact on the recD and hsdS G4s, it is important to note that these targets hold considerable biological relevance. We are trying to synthesize new molecules with the aim of targeting and stabilizing these G4s which could potentially lead to a notable reduction in the MIC of *S. pneumoniae* overall. **An4** effectively inhibited *pmrA* expression, in contrast to ciprofloxacin, which had no impact on *pmrA* expression. A GFP-based reporter assay confirmed this inhibition resulted from **An4**'s binding to the *pmrA* G-quadruplex. Moreover, TOF-SIMS analysis revealed **An4**'s ability to enhance the retention of ethidium bromide (EtBr) in a dose-dependent manner. Furthermore, we have achieved bio-orthogonal synthesis of **An4** using *pmrA* G-quadruplex as templates within live bacterial cells. Overall, our study, on G-quadruplex-mediated drug efflux inhibition in *S. pneumoniae*, suggests that DNA G-quadruplexes may play a broader role in bacterial transcriptional regulation and present potential drug targets to address the pressing issue of antibiotic resistance.

Data availability

The data underlying this article are available in the article and in its online supplementary material.

Supplementary data

Supplementary Data are available at NARMME Online.

Acknowledgements

J.D. thanks Wellcome Trust/DBT India Alliance Fellowship [IA/S/18/2/503986], Science and Engineering Research Board [CRG] and Technical Research Centre-IACS for funding. R.C. thanks UGC for a senior research fellowship. T.P. thanks NIPER for senior research fellowship. DB thanks CSIR

for junior research fellowship. We thank Dr. Umesh for helping with SIMS analysis. We thank Prof. V. Ravichandiran, Director, NIPER-Kolkata for giving us access to the Leica DMI8 Stellaris 5 microscope and Shreetoma Kundu for helping with confocal imaging.

Funding

Wellcome Trust/DBT Alliance, India [IA/S/18/2/503986]; Science and Engineering Research Board [CRG].

Conflict of interest statement

None declared.

References

- Spiegel, J., Adhikari, S. and Balasubramanian, S. (2020) The structure and function of DNA G-quadruplexes. *Trends Chem.*, **2**, 123–136.
- Robinson, J., Raguseo, F., Nuccio, S.P., Liano, D. and Di Antonio, M. (2021) DNA G-quadruplex structures: more than simple roadblocks to transcription? *Nucleic Acids Res.*, **49**, 8419–8431.
- Huppert, J.L. (2008) Four-stranded nucleic acids: structure, function and targeting of G-quadruplexes. *Chem. Soc. Rev.*, **37**, 1375–1384.
- Siddiqui-Jain, A., Grand, C.L., Bearss, D.J. and Hurley, L.H. (2002) Direct evidence for a G-quadruplex in a promoter region and its targeting with a small molecule to repress c-MYC transcription. *Proc. Natl. Acad. Sci. U.S.A.*, **99**, 11593–11598.
- Jansson, L.I., Hentschel, J., Parks, J.W., Chang, T.R., Lu, C., Baral, R., Bagshaw, C.R. and Stone, M.D. (2019) Telomere DNA G-quadruplex folding within actively extending human telomerase. *Proc. Natl. Acad. Sci. U.S.A.*, **116**, 9350–9359.
- Carvalho, J., Mergny, J.-L., Salgado, G.F., Queiroz, J.A. and Cruz, C. (2020) G-quadruplex, friend or foe: the role of the G-quartet in anticancer strategies. *Trends Mol. Med.*, **26**, 848–861.
- Zhang, R., Shu, H., Wang, Y., Tao, T., Tu, J., Wang, C., Mergny, J.-L. and Sun, X. (2023) G-quadruplex structures are key modulators of somatic structural variants in cancers. *Cancer Res.*, **83**, 1234–1248.
- Cebrián, R., Belmonte-Reche, E., Pirota, V., de Jong, A., Morales, J.C., Freccero, M., Doria, F. and Kuipers, O.P. (2022) G-Quadruplex DNA as a target in pathogenic bacteria: efficacy of an extended naphthalene diimide ligand and its mode of action. *J. Med. Chem.*, **65**, 4752–4766.
- Shankar, U., Jain, N., Mishra, S.K., Sharma, T.K. and Kumar, A. (2020) Conserved G-quadruplex motifs in gene promoter region reveals a novel therapeutic approach to target multi-drug resistance *Klebsiella pneumoniae*. *Front. Microbiol.*, **11**, 1269.
- Murat, P., Zhong, J., Lekieffre, L., Cowieson, N.P., Clancy, J.L., Preiss, T., Balasubramanian, S., Khanna, R. and Tellam, J. (2014) G-quadruplexes regulate Epstein-Barr virus-encoded nuclear antigen 1 mRNA translation. *Nat. Chem. Biol.*, **10**, 358–364.
- Cahoon, L.A. and Seifert, H.S. (2009) An alternative DNA structure is necessary for pilin antigenic variation in *Neisseria gonorrhoeae*. *Science*, **325**, 764–767.
- Thakur, R.S., Desingu, A., Basavaraju, S., Subramanya, S., Rao, D.N. and Nagaraju, G. (2014) *Mycobacterium tuberculosis* DinG is a structure-specific helicase that unwinds G4 DNA: implications for targeting G4 DNA as a novel therapeutic approach. *J. Biol. Chem.*, **289**, 25112–25136.
- Beaume, N., Pathak, R., Yadav, V.K., Kota, S., Misra, H.S., Gautam, H.K. and Chowdhury, S. (2013) Genome-wide study predicts promoter-G4 DNA motifs regulate selective functions in bacteria: radioreistance of *D. radiodurans* involves G4 DNA-mediated regulation. *Nucleic Acids Res.*, **41**, 76–89.

14. Tassinari, M., Zuffo, M., Nadai, M., Pirota, V., Sevilla Montalvo, A.C., Doria, F., Freccero, M. and Richter, S.N. (2020) Selective targeting of mutually exclusive DNA G-quadruplexes: HIV-1 LTR as paradigmatic model. *Nucleic Acids Res.*, **48**, 4627–4642.
15. Xu, H. and Hurley, L.H. (2022) A first-in-class clinical G-quadruplex-targeting drug. The bench-to bedside translation of the fluoroquinolone QQ58 to CX-5461 (Pidnarulex). *Bioorg. Med. Chem. Lett.*, **77**, 129016.
16. Rota Sperti, F., Dupouy, B., Mitteaux, J., Pipier, A., Pirrotta, M., Chéron, N., Valverde, I.E. and Monchaud, D. (2022) Click-chemistry-based biomimetic ligands efficiently capture G-quadruplexes in vitro and help localize them at DNA damage sites in human cells. *JACS Au*, **2**, 1588–1595.
17. Piazza, A., Boule, J.-B., Lopes, J., Mingo, K., Largy, E., Teulade-Fichou, M.-P. and Nicolas, A. (2010) Genetic instability triggered by G-quadruplex interacting Phen-DC compounds in *Saccharomyces cerevisiae*. *Nucleic Acids Res.*, **38**, 4337–4348.
18. Perrone, R., Lavezzo, E., Riello, E., Manganeli, R., Palù, G., Toppo, S., Provvedi, R. and Richter, S.N. (2017) Mapping and characterization of G-quadruplexes in *Mycobacterium tuberculosis* gene promoter regions. *Scientific Rep.*, **7**, 5743.
19. Cebrian, R., Belmonte-Reche, E., Pirota, V., de Jong, A., Morales, J.C., Freccero, M., Doria, F. and Kuipers, O.P. (2022) G-Quadruplex DNA as a target in pathogenic bacteria: efficacy of an extended naphthalene diimide ligand and its mode of action. *J. Med. Chem.*, **65**, 4752–4766.
20. Mishra, S.K., Shankar, U., Jain, N., Sikri, K., Tyagi, J.S., Sharma, T.K., Mergny, J.-L. and Kumar, A. (2019) Characterization of G-quadruplex motifs in espB, espK, and cyp51 genes of *Mycobacterium tuberculosis* as potential drug targets. *Mol. Ther. Nucleic Acids*, **16**, 698–706.
21. Shitikov, E., Bespiatykh, D., Malakhova, M., Bespiatykh, J., Bodoev, I., Vedekhina, T., Zaychikova, M., Veselovsky, V., Klimina, K. and Ilna, E. (2022) Genome-wide transcriptional response of *Mycobacterium smegmatis* MC2155 to G-quadruplex ligands BRACO-19 and TMPyP4. *Front. Microbiol.*, **13**, 817024.
22. File, T.M. (2003) Community-acquired pneumonia. *Lancet*, **362**, 1991–2001.
23. Mishra, S.K., Jain, N., Shankar, U., Tawani, A., Sharma, T.K. and Kumar, A. (2019) Characterization of highly conserved G-quadruplex motifs as potential drug targets in *Streptococcus pneumoniae*. *Scientific Rep.*, **9**, 1791.
24. Gill, M.J., Brenwald, N.P. and Wise, R. (1999) Identification of an efflux pump gene, pmrA, associated with fluoroquinolone resistance in *Streptococcus pneumoniae*. *Antimicrob. Agents Chemother.*, **43**, 187–189.
25. Zeller, V., Janoir, C., Kitzis, M.-D., Gutmann, L. and Moreau, N.J. (1997) Active efflux as a mechanism of resistance to ciprofloxacin in *Streptococcus pneumoniae*. *Antimicrobial Agents Chemother.*, **41**, 1973–1978.
26. Li, J., Li, J.-W., Feng, Z., Wang, J., An, H., Liu, Y., Wang, Y., Wang, K., Zhang, X. and Miao, Z. (2016) Epigenetic switch driven by DNA inversions dictates phase variation in *Streptococcus pneumoniae*. *PLoS Pathogens*, **12**, e1005762.
27. Dillingham, M.S. and Kowalczykowski, S.C. (2008) RecBCD enzyme and the repair of double-stranded DNA breaks. *Microbiol. Mol. Biol.*, **72**, 642–671.
28. Meek, R.W., Vyas, H. and Piddock, L.J.V. (2015) Nonmedical uses of antibiotics: time to restrict their use? *PLoS Biology*, **13**, e1002266.
29. Alcock, B.P., Raphenya, A.R., Lau, T.T., Tsang, K.K., Bouchard, M., Edalatmand, A., Huynh, W., Nguyen, A.-L.V., Cheng, A.A. and Liu, S. (2020) CARD 2020: antibiotic resistance surveillance with the comprehensive antibiotic resistance database. *Nucleic Acids Res.*, **48**, D517–D525.
30. Harris, L.M. and Merrick, C.J. (2015) G-quadruplexes in pathogens: a common route to virulence control? *PLoS Pathogens*, **11**, e1004562.
31. Ligozzi, M., Bernini, C., Bonora, M.G., De Fatima, M., Zuliani, J. and Fontana, R. (2002) Evaluation of the VITEK 2 system for identification and antimicrobial susceptibility testing of medically relevant gram-positive cocci. *J. Clin. Microbiol.*, **40**, 1681–1686.
32. Savanur, H.M., Naik, K.N., Ganapathi, S.M., Kim, K.M. and Kalkhambkar, R.G. (2018) Click chemistry inspired design, synthesis and molecular docking studies of coumarin, quinolinone linked 1, 2, 3-triazoles as promising anti-microbial agents. *Chem. Select*, **3**, 5296–5303.
33. Coelho, T., Machado, D., Couto, I., Maschmann, R., Ramos, D., von Groll, A., Rossetti, M.L., Silva, P.A. and Viveiros, M. (2015) Enhancement of antibiotic activity by efflux inhibitors against multidrug resistant *Mycobacterium tuberculosis* clinical isolates from Brazil. *Front. Microbiol.*, **6**, 330.
34. De Cian, A., Guittat, L., Kaiser, M., Saccà, B., Amrane, S., Bourdoncle, A., Alberti, P., Teulade-Fichou, M.-P., Lacroix, L. and Mergny, J.-L. (2007) Fluorescence-based melting assays for studying quadruplex ligands. *Methods*, **42**, 183–195.
35. Jacobi, C., Roggenkamp, A., Rakin, A., Zumbihl, R., Leitritz, L. and Heesemann, J. (1998) In vitro and in vivo expression studies of yopE from *Yersinia enterocolitica* using the gfp reporter gene. *Mol. Microbiol.*, **30**, 865–882.
36. Kumari, S., Bugaut, A., Huppert, J.L. and Balasubramanian, S. (2007) An RNA G-quadruplex in the 5' UTR of the NRAS proto-oncogene modulates translation. *Nat. Chem. Biol.*, **3**, 218–221.
37. Lanni, E.J., Masyuko, R.N., Driscoll, C.M., Aerts, J.T., Shrout, J.D., Bohn, P.W. and Sweedler, J.V. (2014) MALDI-guided SIMS: multiscale imaging of metabolites in bacterial biofilms. *Analyt. Chem.*, **86**, 9139–9145.
38. Saxon, E. and Bertozzi, C.R. (2000) Cell surface engineering by a modified Staudinger reaction. *Science*, **287**, 2007–2010.
39. Siegrist, M.S., Whiteside, S., Jewett, J.C., Aditham, A., Cava, F. and Bertozzi, C.R. (2013) D-amino acid chemical reporters reveal peptidoglycan dynamics of an intracellular pathogen. *ACS Chem. Biol.*, **8**, 500–505.
40. Geva-Zatorsky, N., Alvarez, D., Hudak, J.E., Reading, N.C., Erturk-Hasdemir, D., Dasgupta, S., Von Andrian, U.H. and Kasper, D.L. (2015) In vivo imaging and tracking of host-microbiota interactions via metabolic labeling of gut anaerobic bacteria. *Nat. Med.*, **21**, 1091–1100.
41. Saxon, E., Luchansky, S.J., Hang, H.C., Yu, C., Lee, S.C. and Bertozzi, C.R. (2002) Investigating cellular metabolism of synthetic azidosugars with the Staudinger ligation. *J. Am. Chem. Soc.*, **124**, 14893–14902.
42. Agarwal, P., Beahm, B.J., Shieh, P. and Bertozzi, C.R. (2015) Systemic fluorescence imaging of zebrafish glycans with bioorthogonal chemistry. *Angew. Chem.*, **127**, 11666–11672.
43. Rangan, K.J., Yang, Y.-Y., Charron, G. and Hang, H.C. (2010) Rapid visualization and large-scale profiling of bacterial lipoproteins with chemical reporters. *J. Am. Chem. Soc.*, **132**, 10628–10629.
44. Neef, A.B. and Schultz, C. (2009) Selective fluorescence labeling of lipids in living cells. *Angew. Chem. Int. Ed.*, **48**, 1498–1500.
45. Neef, A.B. and Luedtke, N.W. (2011) Dynamic metabolic labeling of DNA in vivo with arabinosyl nucleosides. *Proc. Natl. Acad. Sci. U.S.A.*, **108**, 20404–20409.
46. Liechti, G., Kuru, E., Hall, E., Kalinda, A., Brun, Y., VanNieuwenhze, M. and Maurelli, A. (2014) A new metabolic cell-wall labelling method reveals peptidoglycan in *Chlamydia trachomatis*. *Nature*, **506**, 507–510.
47. Bublitz, D.C., Chadwick, G.L., Magyar, J.S., Sandoz, K.M., Brooks, D.M., Mesnage, S., Ladinsky, M.S., Garber, A.I., Bjorkman, P.J. and Orphan, V.J. (2019) Peptidoglycan production by an insect-bacterial mosaic. *Cell*, **179**, 703–712.
48. Chaudhuri, R., Prasanth, T. and Dash, J. (2023) Expanding the toolbox of target directed bio-orthogonal synthesis: in situ direct macrocyclization by DNA templates. *Angew. Chem., Int. Ed.*, **62**, e202215245.